

Novel algorithm of large-scale simultaneous linear equations

This article has been downloaded from IOPscience. Please scroll down to see the full text article.

2010 J. Phys.: Condens. Matter 22 074206

(<http://iopscience.iop.org/0953-8984/22/7/074206>)

View [the table of contents for this issue](#), or go to the [journal homepage](#) for more

Download details:

IP Address: 129.252.86.83

The article was downloaded on 30/05/2010 at 07:08

Please note that [terms and conditions apply](#).

Novel algorithm of large-scale simultaneous linear equations

T Fujiwara^{1,2}, T Hoshi^{2,3}, S Yamamoto^{2,4}, T Sogabe⁵ and S-L Zhang⁵

¹ Center for Research and Development of Higher Education, The University of Tokyo, Bunkyo-ku, Tokyo, 113-8656, Japan

² Core Research for Evolutional Science and Technology, Japan Science and Technology Agency (CREST-JST), Japan

³ Department of Applied Mathematics and Physics, Tottori University, Tottori 680-8550, Japan

⁴ School of Computer Science, Tokyo University of Technology, Katakura-machi, Hachioji City, Tokyo 192-0982, Japan

⁵ Department of Computational Science and Engineering, Nagoya University, Furo-cho, Chikusa-ku, Nagoya 464-8603, Japan

Received 30 May 2009, in final form 15 July 2009

Published 3 February 2010

Online at stacks.iop.org/JPhysCM/22/074206

Abstract

We review our recently developed methods of solving large-scale simultaneous linear equations and applications to electronic structure calculations both in one-electron theory and many-electron theory. This is the shifted COCG (conjugate orthogonal conjugate gradient) method based on the Krylov subspace, and the most important issue for applications is the shift equation and the seed switching method, which greatly reduce the computational cost. The applications to nano-scale Si crystals and the double orbital extended Hubbard model are presented.

1. Introduction: Physics and linear equations

Solving the electronic properties in materials should start by obtaining eigenvalues and eigenvectors of the electronic structures in those materials:

$$H|\alpha\rangle = E|\alpha\rangle \quad (1)$$

$$(z - H)|x^{(j)}\rangle = |j\rangle \quad (2)$$

$$G_{ij}(z) = \langle i|(z - H)^{-1}|j\rangle = \langle i|x^{(j)}\rangle, \quad (3)$$

where H is the Hamiltonian of one-electron problem in a potential field determined self-consistently within the local density approximation of the density functional theory, and $|i\rangle$ and $|j\rangle$ are given states. $G_{ij}(z)$ is the Green's function. A parameter z is a complex number $z = E + i\delta$, E is an energy and δ is an infinitesimal small (positive) number.

The electron–electron interaction is very crucial for many physical properties in strongly correlated materials and *single-electron spectra* in many-electron problems can be obtained by the Green's function of the many-electron problem. The Green's function in the many-electron problem can be defined, once we know the ground state $|\mathcal{G}\rangle$, as

$$G_{ij}(z) = \langle \mathcal{G}|\hat{a}_i(z - H)^{-1}\hat{a}_j^\dagger|\mathcal{G}\rangle, \quad (4)$$

where H is the many-electron Hamiltonian, \hat{a}_i and \hat{a}_i^\dagger are annihilation and creation operators of an electron at the i state (or orbital). Then if we define

$$|j\rangle = \hat{a}_j^\dagger|\mathcal{G}\rangle \quad (5)$$

$$\langle i| = \langle \mathcal{G}|\hat{a}_i, \quad (6)$$

the Green's function can be written in the exactly same form as equations (2) and (3):

$$(z - H)|x^{(j)}\rangle = |j\rangle \quad (7)$$

$$G_{ij}(z) = \langle i|x^{(j)}\rangle. \quad (8)$$

Equations (2) and (7) can be written in a unified form as

$$A\mathbf{x} = \mathbf{b}, \quad A = z - H. \quad (9)$$

We should note that the ground state $|\mathcal{G}\rangle$ of the many-electron problem can also be obtained with the help of equation (9) and the CG method.

Our problem here is how to solve equation (9) if the matrix size of A is huge. The structure of the present paper is as follows. In section 2, the idea of the Krylov subspace

is introduced. We explain the COCG method with shift equations and the seed switching in section 3. Applications to one-electron problems and the extended Hubbard model are presented in section 4, and the conclusions are given in section 5.

2. Krylov subspace method

2.1. Numerical recipe of simultaneous linear equations

Many problems can be reduced to obtaining numerical solutions of a set of large-scale simultaneous linear equations:

$$A\mathbf{x} = \mathbf{b}, \quad A = z - H. \quad (10)$$

There are two categories of solving methods for equation (10).

The first is a *direct method* such as the Gaussian elimination method or the Cholesky decomposition method. The second is an *iterative method*, which is appropriate to a large sparse matrix H . Examples are the *conjugate gradient* (CG) method or Lanczos method.

A very primitive iterative method is the Gram–Schmidt *orthogonalization* method for a set of vectors $\{\mathbf{x}_0, \mathbf{x}_1, \mathbf{x}_2, \dots, \mathbf{x}_{n-1}\}$. Applying the Gram–Schmidt orthogonalization method to a set of vectors $\{\mathbf{x}_0, H\mathbf{x}_0, H^2\mathbf{x}_0, \dots, H^{n-1}\mathbf{x}_0\}$, one can construct the *Krylov subspace* $\mathcal{K}_n(H, \mathbf{x}_0)$ generated from H and \mathbf{x}_0 as

$$\mathcal{K}_n(H, \mathbf{x}_0) = \text{span}\{\mathbf{x}_0, H\mathbf{x}_0, H^2\mathbf{x}_0, \dots, H^{n-1}\mathbf{x}_0\}. \quad (11)$$

Lanczos found a new powerful way to generate an orthogonal basis for such subspace when the matrix is symmetric [1], and this method is related to the Krylov subspace. Hestenes and Stiefel proposed the conjugate gradient (CG) method for systems that are both symmetric and positive definite [2].

2.2. Krylov subspace

When H is a huge $N \times N$ matrix, the inverse of H is not easily obtained, or impossible to obtain, and the iterative method becomes a useful concept.

The condition of construction of the Krylov subspace is

$$\mathbf{x}_n = \mathbf{x}_0 + \mathbf{z}_n, \quad \mathbf{z}_n \in \mathcal{K}_n(H, \mathbf{r}_0). \quad (12)$$

A residual vector of the n th approximate solution can be written as

$$\mathbf{r}_n = \mathbf{b} - A\mathbf{x}_n = \mathbf{r}_0 - A\mathbf{z}_n, \quad \mathbf{r}_n \in \mathcal{K}_{n+1}(H, \mathbf{r}_0). \quad (13)$$

In order to determine the approximate solution \mathbf{x}_n uniquely, one needs to decide the searching direction of \mathbf{x}_n by an subsidiary condition to the residual vector \mathbf{r}_n . We then adopt the condition of the orthogonal residual condition, which ensures that the iterative procedure can reach an exact solution, at most, after $(N - 1)$ iteration steps.

The basic theorem of the Krylov subspace is the invariance of the subspace under a scalar shift $\sigma \mathbf{1}$:

$$\mathcal{K}_n(H, \mathbf{r}_0) = \mathcal{K}_n(\sigma \mathbf{1} + H, \mathbf{r}_0). \quad (14)$$

3. COCG method

3.1. Hermitian matrix and CG method

When the matrix H is Hermitian, the procedure is the well-known ‘conjugate gradient’ (CG) method [2]. Here an inner product of vectors $\mathbf{u} = (u_1, u_2, \dots, u_N)^T$ and $\mathbf{v} = (v_1, v_2, \dots, v_N)^T$ is defined as

$$(\mathbf{u}, \mathbf{v}) = \mathbf{u}^{*T} \mathbf{v} = \sum_{i=1}^N u_i^* v_i \quad (15)$$

and the orthogonal residual condition in the CG method is

$$\mathbf{r}_n \perp \mathcal{K}_n(H, \mathbf{r}_0). \quad (16)$$

We define \mathbf{x}_n , \mathbf{p}_n and \mathbf{r}_n as the approximate solution at the n th iteration, the searching direction for the solution at the next iteration step, and the residual vector, respectively. Under the initial conditions:

$$\mathbf{x}_0 = \mathbf{p}_{-1} = \mathbf{0}, \quad (17)$$

$$\mathbf{r}_0 = \mathbf{b}, \quad (18)$$

$$\alpha_{-1} = 1, \quad \beta_{-1} = 0, \quad (19)$$

we solve the following equations:

$$\mathbf{x}_n = \mathbf{x}_{n-1} + \alpha_{n-1} \mathbf{p}_{n-1}, \quad (20)$$

$$\mathbf{r}_n = \mathbf{r}_{n-1} - \alpha_{n-1} A \mathbf{p}_{n-1}, \quad (21)$$

$$\mathbf{p}_n = \mathbf{r}_n + \beta_{n-1} \mathbf{p}_{n-1}, \quad (22)$$

$$\alpha_{n-1} = \frac{(\mathbf{r}_{n-1}, \mathbf{r}_{n-1})}{(\mathbf{p}_{n-1}, A \mathbf{p}_{n-1})}, \quad (23)$$

$$\beta_{n-1} = \frac{(\mathbf{r}_n, \mathbf{r}_n)}{(\mathbf{r}_{n-1}, \mathbf{r}_{n-1})}. \quad (24)$$

The vector sets $\{\mathbf{r}_n\}$ and $\{\mathbf{p}_n\}$ satisfy the following relations:

$$(\mathbf{r}_i, \mathbf{r}_j) = 0, \quad i \neq j \quad (\text{orthogonality relation}) \quad (25)$$

$$(\mathbf{p}_i, A \mathbf{p}_j) = 0, \quad i \neq j \quad (\text{conjugacy relation}). \quad (26)$$

The residual vectors $\{\mathbf{r}_0, \mathbf{r}_1, \mathbf{r}_2, \dots\}$ vanish, at most, after $N - 1$ iteration steps, where N is the dimension of the simultaneous linear equations.

3.2. Complex symmetric matrix and the COCG method

In many problems of physics and engineering, the Hamiltonian H is real symmetric and the matrix A is defined as

$$A = z - H, \quad (27)$$

In other words, the off-diagonal part of A is real symmetric and the diagonal elements can be complex.

Here, instead of the definition of the ‘standard’ inner product equation (15), we define the ‘non-standard’ one as

$$(\mathbf{u}, \mathbf{v}) = \mathbf{u}^T \mathbf{v} = \sum_{i=1}^v u_i v_i, \quad (28)$$

and the orthogonal residual condition in the COCG method is

$$\mathbf{r}_n \perp \overline{\mathcal{K}_n(H, \mathbf{r}_0)}, \quad (29)$$

where the ‘overline’ denotes ‘conjugate’.

Then the conjugate orthogonal conjugate gradient (COCG) method can be constructed in a very similar way [3], with the same initial conditions as the CG method $\mathbf{x}_0 = \mathbf{p}_{-1} = \mathbf{0}$, $\mathbf{r}_0 = \mathbf{b}$, $\alpha_{-1} = 1$, and $\beta_{-1} = 0$:

$$\mathbf{x}_n = \mathbf{x}_{n-1} + \alpha_{n-1} \mathbf{p}_{n-1}, \quad (30)$$

$$\mathbf{r}_n = \mathbf{r}_{n-1} - \alpha_{n-1} A \mathbf{p}_{n-1}, \quad (31)$$

$$\mathbf{p}_n = \mathbf{r}_n + \beta_{n-1} \mathbf{p}_{n-1}, \quad (32)$$

$$\alpha_{n-1} = \frac{(\mathbf{r}_{n-1}, \mathbf{r}_{n-1})}{(\mathbf{p}_{n-1}, A \mathbf{p}_{n-1})}, \quad (33)$$

$$\beta_{n-1} = \frac{(\mathbf{r}_n, \mathbf{r}_n)}{(\mathbf{r}_{n-1}, \mathbf{r}_{n-1})}. \quad (34)$$

We should note that, in the procedure of iteration, $(\mathbf{v}, \mathbf{v}) = 0$ can happen even in the case of $\mathbf{v} \neq \mathbf{0}$ because of the non-standard inner product (28). The inequivalence of $(\mathbf{v}, \mathbf{v}) = 0$ and $\mathbf{v} = \mathbf{0}$ means that the α_n or β_{n-1} may be equal to 0 without satisfying $\mathbf{r}_n = \mathbf{0}$. When this occurs before the approximate solution converges, one fails to obtain the approximate solution. However, we have not experienced such a situation. This cannot happen in the CG method and the other part is perfectly identical to the CG method.

A set of residual vectors \mathbf{r}_n forms the ‘orthogonalized’ base. This ‘orthogonality’ is very important for us to understand the theorem of the collinear residual. We can write a set of the recurrence equations in an alternative way as follows:

$$\mathbf{r}_{n+1} = \left(1 + \frac{\beta_{n-1} \alpha_n}{\alpha_{n-1}} - \alpha_n A\right) \mathbf{r}_n - \frac{\beta_{n-1} \alpha_n}{\alpha_{n-1}} \mathbf{r}_{n-1}. \quad (35)$$

Taking the ‘inner product’ between \mathbf{r}_n and the equation (35), we obtain

$$\alpha_n = \frac{(\mathbf{r}_n, \mathbf{r}_n)}{(\mathbf{r}_n, A \mathbf{r}_n) - \frac{\beta_{n-1}}{\alpha_{n-1}} (\mathbf{r}_n, \mathbf{r}_n)}. \quad (36)$$

Then the equations (36), (34) and (35) can produce all the base vectors, \mathbf{r}_k ’s ($k > n$), when α_{n-1} , \mathbf{r}_{n-1} and \mathbf{r}_n are supplied.

3.3. Shifted COCG method

Assuming that A is a complex symmetric matrix $E_{\text{ref}} + i\delta_{\text{ref}} - H$, we should solve the linear simultaneous equation of

$$A \mathbf{x} = \mathbf{b}, \quad (37)$$

and its shifted equation

$$(A + \sigma) \mathbf{x}^\sigma = \mathbf{b}, \quad (38)$$

where $\sigma = (E + i\delta) - (E_{\text{ref}} + i\delta_{\text{ref}})$. We represent quantities q in the shifted system as q^σ .

The most important point of the reduction of the matrix-vector operation is the theorem of the *collinear residual* [4]:

$$\mathbf{r}_n^\sigma = \frac{1}{\pi_n^\sigma} \mathbf{r}_n, \quad (39)$$

where π^σ is a scalar function (actually a polynomial) of σ . Then, once the $\{\mathbf{r}_n\}$ are given, the base set $\{\mathbf{r}_n^\sigma\}$ for the arbitrarily shifted system can be obtained by using scalar multiplication. We obtain the recurrence equations that determines π_n^σ , α_n^σ , β_n^σ , \mathbf{x}_n^σ , and \mathbf{p}_n^σ , from equations (30)–(34), by replacing A by $A + \sigma$, with the same initial conditions:

$$\pi_{n+1}^\sigma = \left(1 + \frac{\beta_{n-1} \alpha_n}{\alpha_{n-1}} + \alpha_n \sigma\right) \pi_n^\sigma - \frac{\beta_{n-1} \alpha_n}{\alpha_{n-1}} \pi_{n-1}^\sigma, \quad (40)$$

$$\alpha_n^\sigma = \frac{\pi_n^\sigma}{\pi_{n+1}^\sigma} \alpha_n, \quad (41)$$

$$\beta_n^\sigma = \left(\frac{\pi_n^\sigma}{\pi_{n+1}^\sigma}\right)^2 \beta_n, \quad (42)$$

$$\mathbf{x}_n^\sigma = \mathbf{x}_{n-1}^\sigma + \alpha_{n-1}^\sigma \mathbf{p}_{n-1}^\sigma \quad (43)$$

$$\mathbf{p}_n^\sigma = \frac{1}{\pi_n^\sigma} \mathbf{r}_n + \beta_{n-1}^\sigma \mathbf{p}_{n-1}^\sigma. \quad (44)$$

These recurrence equations can be solved without time consuming matrix-vector operations. In actual calculations, we need only one matrix-vector product of a real sparse matrix and a complex vector. Each component of the vector equations (40)–(44) can be solved separately, because of an absence of the matrix operation.

The energy shift parameter σ can be a complex number. When one applies the theorem of the collinear residual [4] to the COCG method, the shifted COCG method is constructed [5, 6]. The essential property is based on the basic invariance theorem of the Krylov subspace equation (14) under an energy shift $E_{\text{ref}} + \sigma$ from E_{ref} . A very important fact is that this shift procedure is a scalar linear calculation. The main cost in the calculations is incurred for those of the seed energy E_{ref} ; the rest is a scalar linear calculation which is negligible from the viewpoint of time consumption.

The complex symmetric linear equations can be treated in the QMR_SYM [7] method and the idea of shift equations here is extended to the QMR_SYM method [8].

3.4. Seed switching technique

The choice of the seed energy E_{ref} is not unique and any choice gives the same convergence behavior of the solutions \mathbf{x}_n at any energy point. However, when the seed energy is chosen at an energy point where the convergence is too fast, the exponent of the scale factor π_n^σ sometimes becomes too large ($\pi_n^\sigma \sim 10^{-100}$) for other energy points and may lead to erroneous results. Therefore, the seed energy should be chosen at the energy point where the convergence is the slowest.

Other possibility is the *seed switching* [9, 6]: we can choose the seed energy at an arbitrary energy point. Let us assume that the convergence at the seed energy has been satisfied before the calculation of the shift equations has converged. In such a case, one chooses a new seed energy $E_{\text{ref}}^{\text{new}}$ and continues the calculation with that seed energy, without discarding the information from the previous calculation with the old E_{ref} .

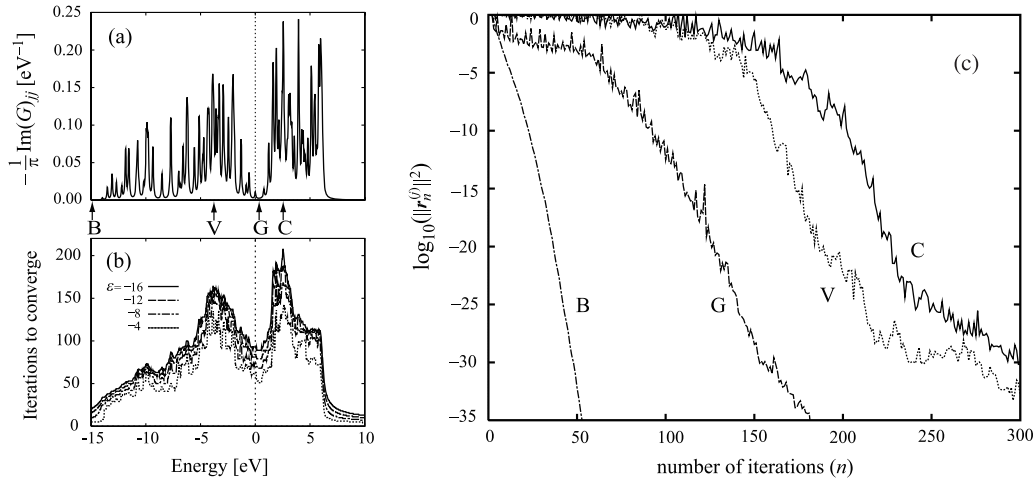


Figure 1. COCG calculation in a Si crystal. (a) Density of states of a Si single crystal with 512 atoms. (b) Convergence behavior at different energies. (c) Iteration dependence of the residual norm. The behavior B, V, G, C corresponds to the energy point in (a).

3.5. Accuracy control with the residual vector and robustness of the shifted COCG method

The residual vector \mathbf{r}_n can be monitored during the iterative calculation and we can stop the iterative procedure, without fixing the dimension of the Krylov subspace, once one reaches the required accuracy. The norm of the residual vector is the upper limit of the accuracy of the Green's function [6]. The shifted COCG method is numerically robust and one can reduce the norm of the residual vector to the machine accuracy. Therefore, the shifted COCG method may be used to calculate an accurate or fine density of electronic states in the electron spectra of large-scale systems or the fine excitation spectra in many-electron problems.

4. Application to nano-scale systems

4.1. Formation and propagation of fracture in a silicon crystal

Nano-scale systems have received much attention and the first principles molecular dynamics simulation has been extending its role in material science and development. We have developed a set of computational methods for electronic structure calculations, i.e. the generalized Wannier state method [10–12], the Krylov subspace method [13], and the shifted COCG method for nano-scale systems [5].

Here we demonstrate a calculation of the electronic structure in bulk Si using the COCG method. We use the tight-binding Hamiltonian by Kwon *et al* [14]. The system is of Si 512 atoms with a cubic simulation cell. (The size of the present Hamiltonian matrix is $(4 \times 512) \times (4 \times 512)$). The imaginary part of the Green's function, corresponding to the density of states, is shown in figure 1(a). Since the $N_{\text{ene}} = 1000$ energy points are selected with a small imaginary part $\delta = 0.002$ au, the spectrum consists of a set of spikes. Figure 1(b) shows the iteration numbers for four cases of the convergence criterion 10^ϵ , from 10^{-4} to 10^{-16} , applied in the COCG method. An energy point with the larger density of states requires the more iterations, because the dimension of the Krylov subspace should be larger in order to distinguish individuals among

densely distributed nearby states. In figure 1(c), we compare the decaying behavior

$$\|\mathbf{r}_n^{(j)}\|^2 = \sum_i |\langle i | \mathbf{r}_n^{(j)} \rangle|^2 = \sum_i |\langle \mathbf{i}, \mathbf{r} \rangle|^2 \quad (45)$$

for chosen energy points B, V, G and C in the band region shown in figure 1(a). Among these energy points, the Green's function calculation converges very rapidly at the energy point B, and those at other energy points are slower. If one choose the seed energy at the point B, one should switch it to other point soon. Even so, the total iteration steps for the convergence over the whole energy range is not sensitive to a choice of a seed energy and the times of seed switching, when we adopt the seed switching technique.

4.2. Excitation spectrum of multi-orbital extended Hubbard model

Strongly correlated electron systems have attracted much attention in both fundamental and applied physics and chemistry. These systems show a drastic change of physical properties with a small change of electron/hole concentration, electric or magnetic field, pressure etc. A stripe order of charge and spin has been found in several layered perovskites and organic conductors. Nickel compound $\text{La}_{2-x}\text{Sr}_x\text{NiO}_4$ is a typical system of stripe order of charge and spin [15–17].

We applied the shifted COCG method to a double orbital extended Hubbard model of the layered perovskite $\text{La}_{3/2}\text{Sr}_{1/2}\text{NiO}_4$ [18, 6], the $\sqrt{8} \times \sqrt{8}$ square lattice of a periodic boundary condition with 12 electrons. The Hamiltonian is as follows:

$$\begin{aligned} \hat{H} = & \sum_{i,j,\alpha,\beta,\sigma} t_{i\alpha j\beta} \hat{c}_{i\alpha\sigma}^\dagger \hat{c}_{j\beta\sigma} + \sum_{i,\alpha,\sigma} \epsilon_{i\alpha} \hat{n}_{i\alpha\sigma} \\ & + U \sum_{i,\alpha} \hat{n}_{i\alpha\uparrow} \hat{n}_{i\alpha\downarrow} + (U - 2J) \sum_{i,\sigma,\sigma'} \hat{n}_{i,3z^2-1,\sigma} \hat{n}_{i,x^2-y^2,\sigma'} \\ & + \frac{J}{2} \sum_{i,\alpha \neq \beta,\sigma,\sigma'} (\hat{c}_{i\alpha\sigma}^\dagger \hat{c}_{i\beta\sigma'}^\dagger \hat{c}_{i\alpha\sigma'} \hat{c}_{i\beta\sigma} + \hat{c}_{i\alpha\sigma}^\dagger \hat{c}_{i\alpha\sigma'}^\dagger \hat{c}_{i\beta\sigma'} \hat{c}_{i\beta\sigma}) \\ & + V \sum_{(i,j),\alpha,\beta,\sigma,\sigma'} \hat{n}_{i\alpha\sigma} \hat{n}_{j\beta\sigma'}, \end{aligned} \quad (46)$$

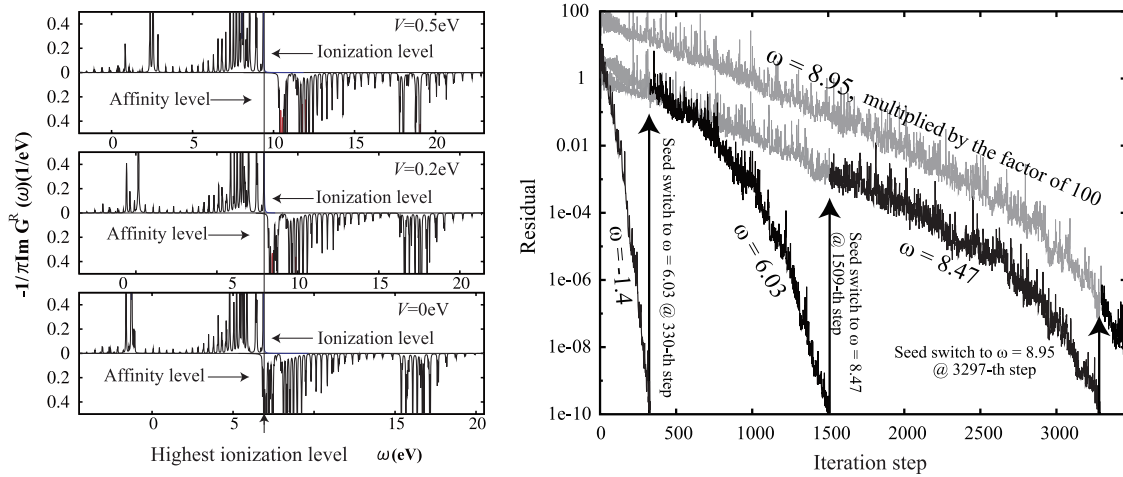


Figure 2. Energy spectra and seed switching in the extended Hubbard model on a two-dimensional square lattice.

Table 1. The values of parameters in the Hamiltonian in units of eV [6, 18]. The prime symbol at the right shoulder of ‘t’ means the second n.n. hopping.

$t_{dd\sigma}$	$t_{dd\delta}$	$\frac{1}{4}t'_{dd\sigma} + \frac{3}{4}t'_{dd\delta}$	$t'_{dd\pi}$	Δ	U	J	V
-0.543	0.058	-0.018	-0.023	0.97	7.5	0.88	0.5

where the suffix $\{i, j\}$, $\{\alpha, \beta\}$ and $\{\sigma, \sigma'\}$ denote the site, the orbitals $3z^2 - 1$ or $x^2 - y^2$, and the spin coordinate, respectively. The annihilation and number operator are \hat{c} and \hat{n} , respectively. The quantities t , ε , U , J , V are the Slater–Koster type hopping parameter, the single-electron energy, the on-site Coulomb interaction, on-site exchange interaction, and intersite Coulomb interaction, respectively. Hopping parameters are finite for nearest neighbor (n.n.) and second n.n. pairs of sites. The braces $\langle \dots \rangle$ means that the two sites enclosed by them are the n.n. sites.

First, the ground state $|\mathcal{G}\rangle$ was searched for by the CG method. We analyzed the effects of V and the anisotropy of the hopping integral between the second n.n. pair. The charge and stripe order of the ground state is investigated in the many-electron wavefunctions. To know whether the ground state is insulating or metallic, the excitation spectra were studied with the help of the shifted COCG method.

The charge gap and order are created by the intersite Coulomb interaction V . Once the charge ordered of Ni ions (Ni^{3+} and Ni^{2+}) exists and, if we introduce a small anisotropy of 0.02 eV of hopping between second n.n. Ni pairs, the spin stripe order is stabilized [18]. We cannot see any difference in the density of states between the second n.n. hopping integrals with/without such a small anisotropy of hopping integral. In the present paper, we choose the isotropic (tetragonal) parameter set shown in table 1. Figure 2(a) shows the change of spectra with changing V and the insulating gap is formed due to finite values of V . We show the seed switching procedure in figure 2(b).

The size of our Hilbert space is $({}_{16}C_6) \times ({}_{16}C_6) = 64\,128\,064$ for the ground state calculation ($S_z = 0$), $({}_{16}C_7) \times ({}_{16}C_6) = 91\,611\,520$ for the affinity level calculation and

$({}_{16}C_5) \times ({}_{16}C_6) = 34\,978\,944$ for the ionization level calculation. This calculation of the sparse matrix-vector product is parallelized and can be accomplished in 1.9 s in the affinity level calculation and 0.5 s in the ionization level calculation by using a one-node (16 CPU) of a modern supercomputer (HITACHI-SR1100).

5. Conclusions

We have reviewed our recently developed methods for large-scale simultaneous linear equations and applications to both one-electron theory and many-electron theory. The most crucial point is that the idea is based on mathematical theory and the accuracy can be monitored and controlled during the calculations. Then we presented examples of the applications to nano-scale Si crystals and the orbital degenerated extended Hubbard model. We would like to stress the importance of this novel computational algorithm in problems of large-scale simultaneous equations.

Acknowledgments

Numerical calculation was partly carried out using the supercomputer facilities of the Institute for Solid State Physics, University of Tokyo. Our research progress on large-scale systems and other information can be found on the WEB page <http://www.elses.jp>.

References

- [1] Lanczos C 1950 *J. Res. Natl Bur. Stand.* **45** 225
Lanczos C 1952 *J. Res. Natl Bur. Stand.* **49** 33
- [2] Hestenes M R and Stiefel E 1952 *J. Res. Natl Bur. Stand.* **49** 409
- [3] van der Vorst H A and Melissen J B M 1990 *IEEE Trans. Magn.* **26** 706
- [4] Frommer A 2003 *Computing* **70** 87
- [5] Takayama R, Hoshi T, Sogabe T, Zhang S-L and Fujiwara T 2006 *Phys. Rev. B* **73** 165108
- [6] Yamamoto S, Sogabe T, Hoshi T, Zhang S-L and Fujiwara T 2008 *J. Phys. Soc. Japan* **77** 114713

- [7] Freund R W 1992 *SIAM J. Sci. Stat. Comput.* **13** 425
- [8] Sogabe T, Hoshi T, Zhang S-L and Fujiwara T 2008 *Electron. Trans. Numer. Anal. (ETNA)* **31** 126
- [9] Sogabe T, Hoshi T, Zhang S-L and Fujiwara T 2007 *Frontiers of Computational Science* ed Y Kaneda, H Kawamura and M Sasai (Berlin: Springer) pp 189–95
- [10] Hoshi T and Fujiwara T 2000 *J. Phys. Soc. Japan* **69** 3773
- [11] Hoshi T and Fujiwara T 2003 *J. Phys. Soc. Japan* **72** 2429
- [12] Hoshi T, Iguchi Y and Fujiwara T 2005 *Phys. Rev. B* **72** 075323
- [13] Takayama R, Hoshi T and Fujiwara T 2004 *J. Phys. Soc. Japan* **73** 1519
- [14] Kwon I, Biswas R, Wang C Z, Ho K M and Soukoulis C M 1994 *Phys. Rev. B* **49** 7242
- [15] Yoshizawa H *et al* 2000 *Phys. Rev. B* **61** R854
- [16] Kajimoto R, Ishizaka K, Yoshizawa H and Tokura Y 2003 *Phys. Rev. B* **67** 014511
- [17] Cava R J, Batlogg B, Palstra T T, Krajewski J J, Peck W F Jr, Ramirez A P and Rupp L W Jr 1991 *Phys. Rev. B* **43** 1229
- [18] Yamamoto S, Fujiwara T and Hatsugai Y 2007 *Phys. Rev. B* **76** 165114